



# Influence of $Al_5FeSi$ Phases on the Cracking of Castings at Al-Si Alloys

I. Hren \*, J. Svobodova, Š. Michna

Faculty of Mechanical Engineering, Institute of Technology and Materials, University of J. E. Purkyně  
in Ústí nad Labem, Pasteurova 7, 400 96 Ústí nad Labem. Czech Republic

\* Corresponding author. E-mail address: Iryna.hren@ujep.cz

Received 21.08.2018; accepted in revised form 30.11.2018

## Abstract

The research described in this contribution is focused on fractographic analysis of the fracture area of newly developed eutectic silumin type  $AlSi9NiCuMg0.5$  (AA 4032), which was developed and patented by a team of staff of the Faculty of Mechanical Engineering. The paper presents determination of the cause of casting cracks in operating conditions. Fractographic analysis of the fracture area, identification of the structure of the casting, identification of structural components on the surface of the fracture surface and chemical analysis of the material in the area of refraction were performed within the experiment. Al-Si alloys with high specific strength, low density, and good castability are widely used in pressure-molded components for the automotive and aerospace industries. The results shown that the inter-media phases Fe-Al and Fe-Si in aluminium alloys lead to breakage across the entire casting section and a crack that crossed the entire cross section, which was confirmed by EDS analysis.

**Keywords:** Aluminium alloy, Intermetallic phase, Low pressure casting, Structure, Iron contamination

## 1. Introduction

Iron is an element we always find in aluminium and its alloys. The melt is obtained in a variety of ways, for example, by fowl the batch of melting iron, steel tools used in the melting and casting process, dissolving the steel or cast iron parts of the apparatus, etc. Iron is therefore most commonly found in aluminium alloys as impurities. In some cases, Fe is added to aluminium alloys as an alloying element. If the iron is an alloying element, its content in aluminium alloys typically does not exceed 1.0 weight percent. Iron in the form of an alloying element improves the strength properties at higher alloy strengths and increases its hardness at the expense of a considerable reduction in elongation. Iron mainly causes corrosion resistance (point corrosion), reduces thermal and electrical conductivity [1, 2]. Iron has low solubility in aluminium alloys and is eliminated as intermetallic phases. The intermetallic phases are for example  $FeAl_6$ ,  $FeAl_3$ ,  $Fe_2SiAl_8$ ,  $AlFeMnSi$  and

$Al_5FeSi$ . At an iron content above 0.6 wt. % of  $Al_5FeSi$  brittle phases begin to prevail, which are eliminated in the sub-eutectic siluminates in the interventricular spaces. These phases significantly reduce the plastic properties of the material [3, 4, 5].

The AA 4032 eutectic silumin alloy was prepared under operating conditions developed and patented by a team of workers at the Faculty of Mechanical Engineering for low pressure technology. Castings were made by low-light casting technology. In casting technology, the melt is fed into the mould cavity via a cast iron filler pipe.

The goal is to improve bonding and achieve higher heat resistance (up to 200 °C) for the resulting castings. The chemical composition of the patented alloy is shown in Tab. 1.

The batch was prepared from the 60% batch of purchased batch and the remainder was a porter waste which already carries an increased iron content from the previous calculations. After melting the batch, the alumina was treated with the refining salt

and refined with argon for 5 min. Argon refining was performed with strontium modification in the form of wire.

The next step is moulding at a temperature of 745 °C on a low-pressure die-casting device having a pressure of 0.3 MPa.

The ascending tube, with dimensions of 30x5 cm, is made of cast iron.

Table 1.

The chemical composition of AA 4032 alloy

Element	Si	Fe	Cu	Mn	Mg	Cr	Zn	Sr	Ti	Al
Amount [wt. %]	8.5-10.0	max. 0.7	0.6-1.0	max. 0.6	0.4-0.8	max.0.15	max. 0.1	0.02-0.05	max. 0.15	balance

When cast casts were used, they were cracked in the entire cross section. On the overall fracture area of the casting are visible glossy surfaces which are take about 20% of the fracture area (Figure 1).

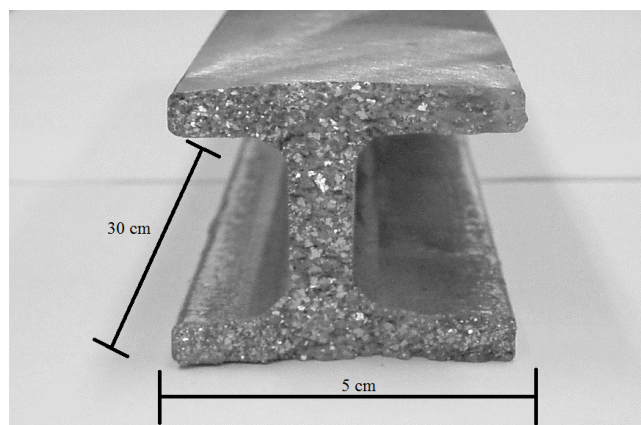


Fig. 1. Total casting surface, mag. 3x

## 2. Chemical composition of casting

Spectral chemical analysis of the casting was carried out on an optical emission spectrometer Q4 TASMAN. In a cast were performed 5 measuring on an area near the fracture.

From these measurements the average value was determined for individual elements (Table 2).

Compared to the desired composition (Table 1), the chemical composition of the casting in the refractory region shows a high iron content (2.32 wt. %) which is inadmissible in terms of its negative influence on the mechanical and chemical properties of the alloy [6, 8-10]. For all other elements, the chemical composition corresponds to the required composition of the patented AA 4032 alloy (Table 1).

From the point of view of the desired chemical composition, it is a polycomponent aluminium alloy type AA 4032. The alloy is alloyed with several elements to provide the required material properties.

The basic alloying element is silicon, nickel, copper and magnesium. As a further element, strontium is added, which acts as a modifier. The main alloying element is iron containing up to 0.7 wt. %. For real-world alloys in operation, the Fe content exceeds almost 3 times that of the patented alloy.

Table 2.

The chemical composition of AA 4032 cast alloy

Element	Si	Fe	Cu	Mn	Mg	Cr	Zn	Sr	Ti	Al
Amount [wt. %]	9.23	2.32	0.64	0.42	0.51	0.13	0.023	0.02	0.063	balance

## 3. Results and discussion

### 3.1 Microscopic Structure Assessment

The confocal laser microscope Olympus LEXT OLS 3100 was used to analyse the microstructure of the samples. From the point of view of the overall structure evaluation in the area of the adjacent fracture it can be stated that it is eutectic silumin with a plurality of individual types of structural components. The basic components of the microstructure are  $\alpha$  - solid solution and silicon in the form of finer and coarse hexagonal plates, which appear in the plane of the metallographic cut as sharp or partially rounded non - regular needles of different size [7, 11, 12]. In the microstructure of AA 4032 alloy, within the analysis, measurements were made and particles were found with a size in the range of 10 - 40  $\mu\text{m}$  (marked by arrow on Figure 2 ). This

suggests that the shape of the eutectic silicon emitted begins to change from plate to bar-shaped or fibre-shaped, where the strontium content of the silicon is insufficient [13]. In addition, because of the high iron content, there are visible rough intermetallic phases of the  $\text{Al}_3\text{FeSi}$  type size approximately 160-400  $\mu\text{m}$  (Figure 2 and Figure 4). Part of the intermetallic phases of the  $\text{Al}_3\text{FeSi}$  type are also crystallized in the form of irregular multiform shape-like formations (marked by arrow on Figure 4). In the microstructure, we can see the intermetallic phases of  $\text{AlFe}(\text{Si})\text{Mn}$  type Chinese script 100-300  $\mu\text{m}$  (marked by arrow on Figure 3).

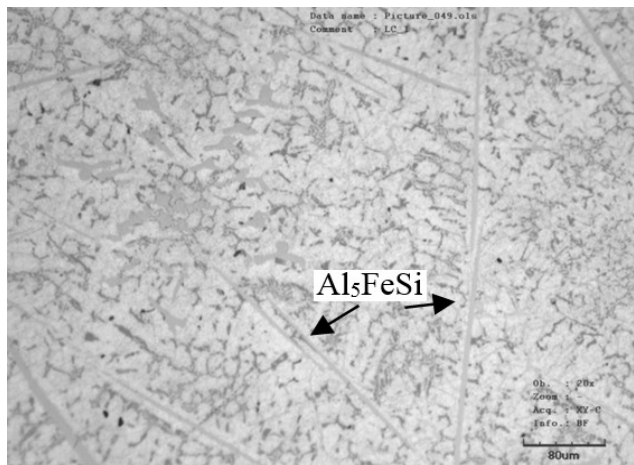


Fig. 2. Microstructure of AA 4032 alloy with brittle intermetallic phases of the  $Al_5FeSi$

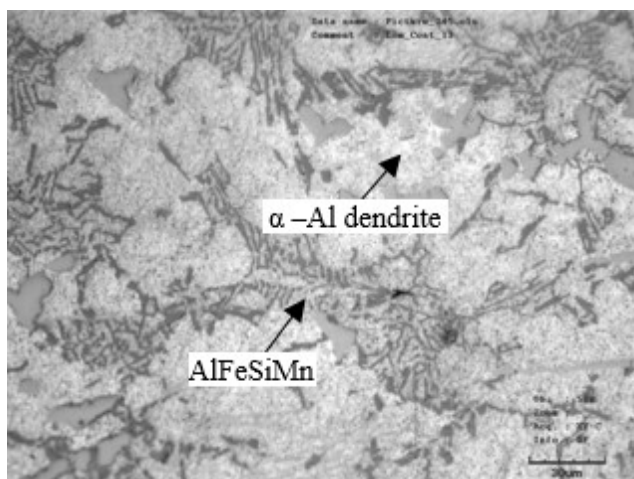


Fig. 3. Area of microstructure of AA4032 alloy with intermetallic phases of  $AlFeSiMn$  type Chinese script

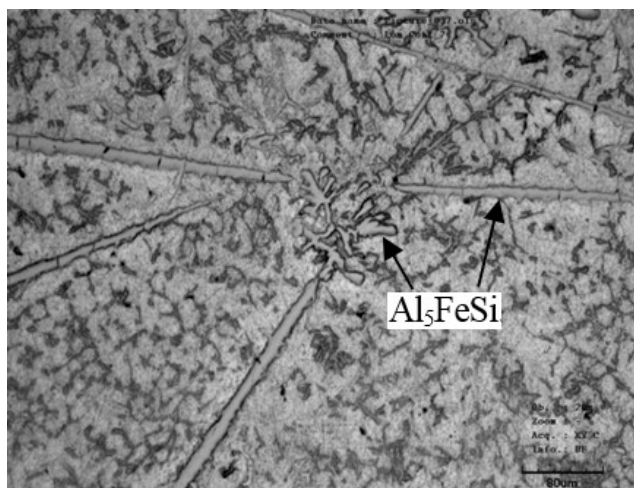


Fig. 4. Morphology of Fe-rich intermetallic phases in as-cast structure of AA 4032 alloy

The fracture microstructure in the fracture area shows a fracture breakage (marked by arrow on Figure 5) of brittle intermetallic phases of the  $Al_5FeSi$  type, which initiate material breakage.



Fig. 5. Cross section of fractured surfaces of AA 4032 alloy showing fracture mechanism of  $Al_5FeSi$  intermetallic phase

### 3.2 Fractographic analysis of the fracture area

#### Fractographic analysis in place 1.

The surface EDS analysis of the light glossy surfaces (Figure 6) of the fracture break on the fracture surface shows the presence of Al, Fe and Si, where the stoichiometric ratio can be said to be brittle intermetallic phases of type  $Al_5FeSi$ . Spectrum of analysed chemical elements of the S1 area EDS analysis is shown at Figure 7. Quantification of field EDS analysis results are in Table 3. A large number of these brittle intermetallic phases at the fracture area initiate their fission breakdown and cause total cracking and crack propagation across the entire cross section of the casting.

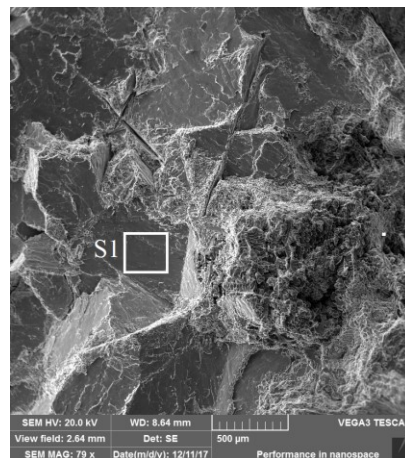


Fig. 6. Area analysis of the sample

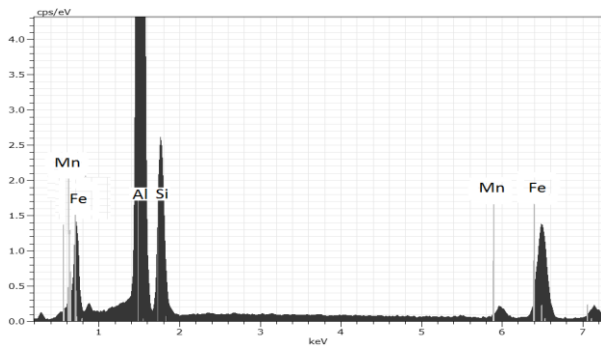


Fig. 7. Spectrum of analysed chemical elements

 Table 3.  
 Quantification of field EDS analysis results

Element	norm. C [wt.%]	Atom. C [at. %]
Aluminium	56.88	50.65
Iron	9.64	4.15
Silicon	12.87	11.01
Magnesium	0.56	0.56
Manganese	2.74	1.20
	100.00	100.00

The surface EDS analysis in the marked area (Figure 8) on the fracture surface shows the presence of Al, Fe, Mn and Si where, in terms of the stoichiometric ratio, it can be deduced that the intermetallic phases of the AlFeSiMn type are found. Spectrum of analysed chemical elements of the S2 area EDS analysis is shown at Figure 9. Quantification of this field EDS analysis results are in Table 4. The presence of oxygen and carbon is related to surface oxidation and partial contamination of the fracture area. Contamination of oxygen and carbon in the alloy will be eliminated in the following cleaning processes.

### Fractographic analysis in place 2.

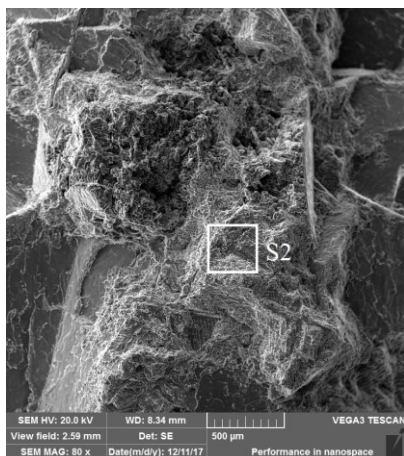


Fig. 8 Area analysis of the sample

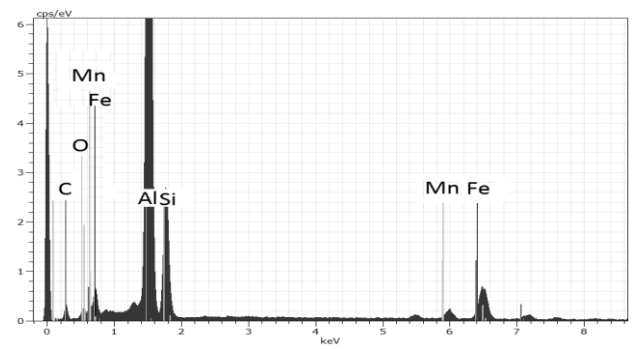


Fig. 9 Spectrum of analysed chemical elements

 Table 4.  
 Quantification of field EDS analysis results

Element	norm. C [wt.%]	Atom. C [at. %]
Aluminium	58.07	48.65
Iron	6.95	2.81
Silicon	10.75	8.66
Manganese	2.75	1.13
Oxygen	3.58	5.05
Carbon	17.91	33.70
	100.00	100.00

The surface EDS analysis of light glossy surfaces (Figure 10) shows the presence of Al, Fe and Si, where the stoichiometric ratio can be said to be fragile intermetallic phases of type  $Al_3FeSi$ . Spectrum of analysed chemical elements of the S3 area EDS analysis is shown at Figure 11. A large number of these brittle intermetallic phases at the fracture area initiate their fission breakdown and cause total cracking and crack propagation across the entire cross section of the casting. The presence of oxygen and carbon, that are shown in Table 5, is related to surface oxidation and contamination of the fracture area, that will be eliminated in the following cleaning processes.

### Fractographic analysis in place 3.

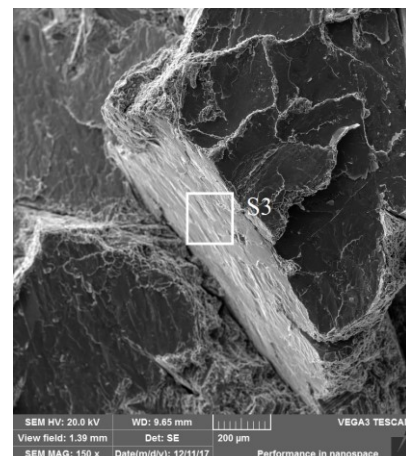


Fig. 10 Area analysis of the sample

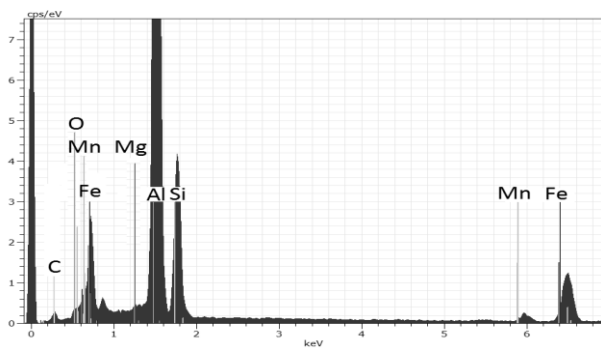


Fig. 11 Spectrum of analysed chemical elements

Table 5.  
Quantification of field EDS analysis results

Element	norm. C [wt.%]	Atom. C [at. %]
Aluminium	56.88	50.65
Iron	9.64	4.15
Silicon	12.87	11.01
Manganese	2.74	1.20
Magnesium	0.56	0.56
Oxygen	4.34	6.52
Carbon	12.96	25.92
	100.00	100.00

## 4. Conclusions

Spectral chemical analysis of the casting (around the fracture) showed a high iron content (up to 2.32 wt. %) over the chemical composition of the patented alloy. Such a high Fe content is unacceptable in terms of its negative influence on the mechanical and chemical properties of the alloy. The required alloy permits the iron content to be the major alloying element of max. 0.7 wt. %. Research and literary sources have shown that for iron contents above 0.6 - 0.7 wt. % (in the absence of Mn), brittle inter-metallic phases of the  $Al_3FeSi$  type occur.

In microstructure analysis, coarse needles (spatially coarse slabs) of brittle intermetallic phases of the  $Al_3FeSi$  type of about 160-400  $\mu m$ , which are associated with high iron content, were identified in the structure. Part of the intermetallic phases of the  $Al_3FeSi$  type is also crystallized in the form of irregular shape-like compact formations. In the microstructure, branched intermetallic phases of  $AlFe(Si)Mn$  of Chinese type are 100-300  $\mu m$ . In addition, the fracture microstructure was investigated. Fragmentation of brittle intermetallic phases of the  $Al_3FeSi$  type, which initiated the material breakdown, was largely observed in the fracture area.

The presence of Al, Fe and Si has been demonstrated by surface EDS analysis of light glossy surfaces in the area of fracture breaking at the fracture surface, where the stoichiometric ratio can be said to be fragile intermetallic phases of type  $Al_3FeSi$ . A large number of these brittle intermetallic phases at the fracture area initiate fission breakdown and cause total cracking and cracking across the entire cross section of the cast. The presence

of oxygen and carbon is related to surface oxidation and partial fracture contamination, which will be eliminated in the following cleaning processes.

From all the analyses and fractographic investigations carried out, it can be stated that the initiator of crack insertion and subsequent cracking of the casting under load is the high content of rough fragments of roughly intermetallic phase of the  $Al_3FeSi$  type on the fracture area (over 20%). The high iron content was due to the dissolution of the cast iron ascension tube by low-pressure casting.

## References

- [1] Michna, Š. et al. (2005). *Encyclopedia of Aluminum*. (1st ed.). Prešov. SR: Adin s. r. o. ISBN 80-89041-88-4. (in Czech).
- [2] Oniszek, A., Rzakosz, S., Wójcik, A. & Cieślak, W. (2007). Iron presence in the technology of Mg-Al casting. *Archives of Foundry Engineering*. 7(2), 19-24.
- [3] Bolibruchová, D., Tillová, E. (2005). *Foundry alloys Al-Si*. ŽU v Žilina – EDIS. ISBN 80-8070-485-6.
- [4] Górný, Z., Kluska Nawarecka, S. & Saja, K. (2013). The Effect of Toughening Combined with Microjet Cooling During Quenching (Solution Heat Treatment) of Calcium Carbide-modified CuAl10Fe4Ni4 Alloy on its Mechanical Properties. *Archives of Foundry Engineering*. 13(1), 29-32.
- [5] Mondolfo, L.F. (1979). *Aluminium Alloys, Structure and Properties*. Butterworths, London.
- [6] Romankiewicz, F. & Romankiewicz, R. (2006). The influence of modification for structure and morphology fractures of alloy AlSi132. *Archives of Foundry*. 6(22), 436-440. (in Polish).
- [7] Lipiński, T. (2011). Microstructure and Mechanical Properties of the AlSi13Mg1CuNi Alloy With Ecological Modifier. *Manufacturing Technology*. 11(11), 40-44. ISBN 1213-2489.
- [8] Lipiński, T. (2008). Improvement of mechanical properties of AlSi7Mg alloy with fast cooling homogenous modifier. *Archives of Foundry Engineering*. 8(1), 85-88.
- [9] Pastircak, R., Sladek, A. & Kucharcikova, E. (2015). The production of plaster molds with patternless process technology. *Archives of Foundry Engineering*. 15(2), 91-94.
- [10] Roskosz, S., Adamiec, J. & Blotnicki, M. (2007). Influence of delivery state quality on microstructure and mechanical properties of as cast AZ91 Mg alloy. *Archives of Foundry Engineering*. 7(1), 143-146.
- [11] Turzyński, J., Pytel, A., Pysz, S. & Żuczek, R. (2006). Improving casting quality through application of modern tools for designing and testing. *Archives of Foundry Engineering*. 6(18), 224-230.
- [12] Cais, J., Svobodova, J. & Stancekova, D. (2017). Modification of the AlSi7Mg0.3 alloy using antimony. *Manufacturing Technology*. 17(5), 685-690.
- [13] Dinnis, C., Taylor, J.A. & Dahle, A.K. (2005). As-cast morphology of iron-intermetallics in Al-Si foundry alloys. *Scripta Materialia*. 53(8), 955-958.